Pure-state tomography with the expectation value of Pauli operators

Xian Ma,[1,2] Tyler Jackson,[1,3] Hui Zhou,[4,5] Jianxin Chen,[6] Dawei Lu,[1,2] Michael D. Mazurek,[1,2] Kent A. G. Fisher,[1,2] Xinhua Peng,[1,4,5] David Kribs,[1,3] Kevin J. Resch,[1,2] Zhengfeng Ji,[1] Bei Zeng,[1,3,7] and Raymond Laflamme[1,2,7,8]

[1]*Institute for Quantum Computing, University of Waterloo, Waterloo, Ontario, Canada N2L 3G1*

[2]*Department of Physics and Astronomy, University of Waterloo, Waterloo, Ontario, Canada N2L 3G1*

[3]*Department of Mathematics & Statistics, University of Guelph, Guelph, Ontario, Canada N1G 2W1*

[4]*Hefei National Laboratory for Physical Sciences at Microscale and Department of Modern Physics, University of Science and Technology of China, Hefei, Anhui 230036, China*

[5]*Synergetic Innovation Center of Quantum Information & Quantum Physics, University of Science and Technology of China, Hefei, Anhui 230026, China*

[6]*Joint Center for Quantum Information and Computer Science, University of Maryland, College Park, Maryland 20742, USA*

[7]*Canadian Institute for Advanced Research, Toronto, Ontario, Canada M5G 1Z8*

[8]*Perimeter Institute for Theoretical Physics, Waterloo, Ontario, Canada N2L 2Y5*

(Received 22 January 2016; published 31 March 2016)

We examine the problem of finding the minimum number of Pauli measurements needed to uniquely determine an arbitrary n-qubit pure state among all quantum states. We show that only 11 Pauli measurements are needed to determine an arbitrary two-qubit pure state compared to the full quantum state tomography with 16 measurements, and only 31 Pauli measurements are needed to determine an arbitrary three-qubit pure state compared to the full quantum state tomography with 64 measurements. We demonstrate that our protocol is robust under depolarizing error with simulated random pure states. We experimentally test the protocol on two- and three-qubit systems with nuclear magnetic resonance techniques. We show that the pure-state tomography protocol saves us a number of measurements without considerable loss of fidelity. We compare our protocol with same-size sets of randomly selected Pauli operators and find that our selected set of Pauli measurements significantly outperforms those random sampling sets. As a direct application, our scheme can also be used to reduce the number of settings needed for pure-state tomography in quantum optical systems.

DOI: 10.1103/PhysRevA.93.032140

I. INTRODUCTION

We consider a d-dimensional Hilbert space $\mathcal{H}_d$, and denote $D(\mathcal{H}_d)$ the set of density operators acting on $\mathcal{H}_d$. Assume that we measure a set of m linearly independent observables

$$\mathbf{A} = (A_0, A_1, A_2, \ldots, A_{m-1}), \tag{1}$$

where each A_i is Hermitian. Without loss of generality, we assume $A_0 = I$ (i.e., the identity operator on $\mathcal{H}_d$), and $\mathrm{tr}\, A_i = 0$ for $i = 1,2,\ldots,m-1$.

Then for any $\rho \in D(\mathcal{H}_d)$, the measurement returns a set of outcomes

$$\boldsymbol{\alpha} = (\mathrm{tr}\,\rho, \mathrm{tr}(\rho A_1), \mathrm{tr}(\rho A_2), \ldots, \mathrm{tr}(\rho A_{m-1})). \tag{2}$$

Theoretically, we always have $\mathrm{tr}\,\rho = 1$; however, we keep this entry in $\boldsymbol{\alpha}$ for the reason of experimental calibration [1–4].

For any $\rho \in D(\mathcal{H}_d)$, full quantum state tomography requires d^2 measurement outcomes to determine ρ [5]. However, for a pure state $|\psi\rangle \in \mathcal{H}_d$, in general only order d measurements are needed to determine $|\psi\rangle$. There is a slight difference in interpreting the term "determine," as clarified in [6] and summarized in the following definition. The physical interpretation in this case is clear: it is useful in quantum tomography to have some prior knowledge that the state to be reconstructed is pure or nearly pure.

Definition 1. A pure state $|\psi\rangle$ is uniquely determined among pure states (UDP) by measuring $\mathbf{A}$ if there does not exist any other pure state which has the same measurement results as those of $|\psi\rangle$ when measuring $\mathbf{A}$. A pure state $|\psi\rangle$ is uniquely determined among all states (UDA) by measuring $\mathbf{A}$ if there does not exist any other state, pure or mixed, which has the same measurement results as those of $|\psi\rangle$ when measuring $\mathbf{A}$.

It is known that there exists a family of $4d-4$ observables such that any d-dimensional pure state is UDP [7], and $5d-6$ observables such that any d-dimensional pure state is UDA [6]. Many other techniques for pure-state tomography have been developed, and experiments have been performed to demonstrate the reduction of the number of measurements needed [8–15]. However, even if there are constructive protocols for the measurement set $\mathbf{A}$, in practice these sets may not be easy to measure in an experiment.

One idea of the compressed sensing protocols as discussed in [16,17] considers measurements of Pauli operators for n-qubit systems, with Hilbert space dimension $d = 2^n$. Since no joint measurements on multiple qubits are needed for Pauli operators, these operators are relatively easy to measure in practice. It is shown that order $d \log d$ random Pauli measurements are sufficient to UDA almost all pure states [18]. That is, all pure states can be determined, up to a set of states with measure zero (i.e., "almost all" pure states are determined). Experiments also demonstrate the usefulness of this method in pure-state tomography in practice [19]. However, it remains open how many Pauli measurements are needed to determine all pure states (UDP or UDA) of an n-qubit system.

In this work, we examine the problem of the minimum number of Pauli operators needed to UDA all n-qubit pure states. For $n = 1$ the number is known to be 3, i.e., all three Pauli operators X, Y, Z are needed. We solve the problem for $n = 2$ and $n = 3$, where at least 11 Pauli operators are

needed for $n = 2$ and at least 31 Pauli operators are needed for $n = 3$. We then demonstrate that our protocol is robust under depolarizing error with simulated random pure states. We further implement our protocol in our nuclear magnetic resonance (NMR) system and compare our result with other methods. As a direct application of this result, we show that our scheme can also be used to reduce the number of settings needed for pure-state tomography in quantum optical systems.

II. PURE-STATE TOMOGRAPHY USING PAULI OPERATORS

We consider the real span of the operators in $\mathbf{A}$, and denote it by $\mathcal{S}(\mathbf{A})$. Let $\mathcal{S}(\mathbf{A})^{\perp}$ be the $(d^2 - m)$-dimensional orthogonal complement subspace of $\mathcal{S}(\mathbf{A})$ inside $\mathbb{R}^{d^2}$. It is known that a sufficient condition for any pure state $|\phi\rangle$ to be UDA by measuring $\mathbf{A}$ is that any nonzero Hermitian operator $H \in (\mathcal{S}(\mathbf{A}))^{\perp}$ have at least two positive and two negative eigenvalues [6]. In fact, this is also a necessary condition. Otherwise, if the second-lowest eigenvalue of H is non-negative, then the two states $|\psi\rangle\langle\psi|$ and $H + |\psi\rangle\langle\psi|$ are indistinguishable by only measuring $\mathbf{A}$ where $|\psi\rangle$ is the eigenvector of H corresponds to the smallest eigenvalue. Note that without loss of generality, we can always assume the smallest eigenvalue of H is greater than -1 which will guarantee $H + |\psi\rangle\langle\psi| \geqslant 0$. A similar argument holds if the second-largest eigenvalue of H is negative. We will then look for such sets $\mathbf{A}$ containing only Pauli operators, for two-qubit and three-qubit pure-state tomography.

A. Two-qubit system

We denote the single-qubit Pauli operators by $\sigma_1 = X, \sigma_2 = Y, \sigma_3 = Z$, and the identity operator $\sigma_0 = I$. For a single qubit, it is straightforward to check that measuring only two of the three operators cannot determine an arbitrary pure state. Therefore, all three Pauli operators are needed in the single-qubit case.

For the two-qubit system, there are a total of 16 Pauli operators, including the identity. These are given by the set $\{\sigma_i \otimes \sigma_j\}$ with $i, j = 0,1,2,3$. For simplicity we omit the tensor product symbol by writing, e.g., XY instead of $X \otimes Y$. Of these 16 Pauli operators, there exists a set of 11 Pauli operators $\mathbf{A}$ such that $\mathbf{A}$ is UDA for any pure state, as given by the following theorem [20].

Theorem 1. Any two-qubit pure state $|\phi\rangle$ is UDA by measuring the following set of Pauli operators:

$$\begin{aligned}\mathbf{A} = \{&II, IX, IY, IZ, XI, YX,\\ &YY, YZ, ZX, ZY, ZZ\},\end{aligned} \tag{3}$$

and no set with fewer than 11 Pauli operators can be UDA for all two-qubit pure states. Moreover, any set of Pauli operators which is Clifford equivalent to $\mathbf{A}$ can be used to UDA for any two-qubit pure states.

This is to say, 11 is the minimum number of Pauli operators needed to UDA any two-qubit pure state, and an example of such a set with 11 Pauli operators is given in Eq. (3).

Proof. In order for $\mathbf{A}$ to UDA all two-qubit pure states it is known [6] that any Hermitian operator $H \in (\mathcal{S}(\mathbf{A}))^{\perp}$ must have at least two positive and two negative eigenvalues.

In this case $(\mathcal{S}(\mathbf{A}))^{\perp} = \mathcal{S}(\{XX, XY, XZ, YI, ZI\})$. Note that the five operators which are not measured all mutually anticommute with each other. It is easy to see that this property is required for if two operators in $(\mathcal{S}(\mathbf{A}))^{\perp}$ commuted, then they would be simultaneously diagonalizable and a linear combination would exist which would have at least one zero eigenvalue. Since two-qubit Pauli operators only have four eigenvalues total, having a single zero eigenvalue fails the UDA condition.

Furthermore, it is easy to show by exhaustive search that there exists no set of more than five mutually anticommuting Pauli operators. So no fewer than 11 Paulis could be measured.

To show that this set of 11 Pauli operators is sufficient to be UDA, we construct a parametrization of all $H \in (\mathcal{S}(\mathbf{A}))^{\perp}$,

$$H = \alpha_1 XX + \alpha_2 XY + \alpha_3 XZ + \alpha_4 YI + \alpha_5 ZI, \tag{4}$$

and show that either H has two positive and two negative eigenvalues or $H = 0$. Note that H then has the following form:

$$\begin{bmatrix} \alpha_5 & 0 & \alpha_3 + \alpha_4 i & \alpha_1 + \alpha_2 i \\ 0 & \alpha_5 & \alpha_1 - \alpha_2 i & -\alpha_3 + \alpha_4 i \\ \alpha_3 - \alpha_4 i & \alpha_1 + \alpha_2 i & -\alpha_5 & 0 \\ \alpha_1 - \alpha_2 i & -\alpha_3 - \alpha_4 i & 0 & -\alpha_5 \end{bmatrix}.$$

The determinant of H can be calculated and the result is

$$\begin{aligned}&\alpha_5^4 + \alpha_5^2|\alpha_3 + \alpha_2 i|^2 + \alpha_5^2|\alpha_1 + \alpha_2 i|^2 + |\alpha_3 - \alpha_4 i|^4\\ &\quad + |\alpha_3 - \alpha_4 i|^2|\alpha_1 + \alpha_2 i|^2 + |\alpha_3 - \alpha_2 i|^2\alpha_5^2 + |\alpha_1 - \alpha_2 i|^4\\ &\quad + |\alpha_1 - \alpha_2 i|^2|\alpha_3 - \alpha_4 i|^2 + |\alpha_1 - \alpha_2 i|^2\alpha_5^2.\end{aligned}$$

This quantity, being the sum of non-negative terms, is greater than or equal to zero. Equality is reached if and only if all terms in the sum are zero, which only occurs when $\alpha_1 = \alpha_2 = \alpha_3 = \alpha_4 = \alpha_5 = 0$. Since H is a 4×4 traceless Hermitian matrix, it can only have positive determinant if and only if it has exactly two positive and two negative eigenvalues.

The same logic follows for any set that is unitarily equivalent to this set. A particular class of unitary operators which maps the set of Pauli operators to itself is called the Clifford group. Thus the set $\mathbf{A}$ and any set which is Clifford equivalent to it are our optimum sets of Pauli measurement operators for two-qubit pure-state tomography.

B. Three-qubit system

The situation for the three-qubit case is much more complicated [20]. We start by noticing that

$$\begin{aligned}V &= IIZ + IZI + ZII + ZZZ\\ &= 4(|000\rangle\langle 000| - |111\rangle\langle 111|)\end{aligned} \tag{5}$$

has one positive and one negative eigenvalue. Therefore, if the set $\mathbf{F}_1 = \{IIZ, IZI, ZII, ZZZ\}$ is a subset of $\mathcal{S}(\mathbf{A})^{\perp}$, the set $\mathbf{A}$ cannot UDA all pure states. Similarly any set $\mathbf{F}_i$ which is Clifford equivalent to $\mathbf{F}_1$ cannot be a subset of $\mathcal{S}(\mathbf{A})^{\perp}$. Sets such as these we call failing sets.

Definition 2. A failing set $\mathbf{F}$ is a set of Pauli operators such that there exists a nonzero real combination of elements chosen from $\mathbf{F}$ such that it has only one positive eigenvalue or one negative eigenvalue.

Namely, for an arbitrary pure state $|\phi\rangle$ to be UDA by measuring operators in a set $\mathbf{A}$, $\text{span}(\mathbf{F}_i) \not\subset (\text{span}(\mathbf{A}))^{\perp}$ holds for every set $\mathbf{F}_i$ that is Clifford equivalent to $\mathbf{F}_1$. Thus, for all 945 sets of $\mathbf{F}_i$, at least one element in each $\mathbf{F}_i$ should be included in $\text{span}(\mathbf{A})$.

Theorem 2. The following set of 31 Pauli operators are sufficient to UDA any given three-qubit pure state $|\phi\rangle$:

$$\begin{aligned}\mathbf{A} = \{&IIX, IIY, IIZ, IXI, IXX, IXY, IYI, IYX,\\ &IYY, IZI, XIZ, XXX, XXY, XYX, XYY,\\ &XZX, XZY, YXX, YXY, YXZ, YYX, YYY,\\ &YYZ, YZI, ZII, ZXZ, ZYZ, ZZX, ZZY,\\ &ZZZ, III\},\end{aligned} \tag{6}$$

and no set with less than 31 Pauli operators can be UDA for all three-qubit pure states. Moreover, any set of Pauli operators which is Clifford equivalent to $\mathbf{A}$ can be used to UDA for any three-qubit pure states.

Similar to the two-qubit case this set is obtained by finding the largest set of Pauli operators which do not contain any of the identified failing sets and taking the complement producing the smallest set of measurement operators which could UDA all pure states.

To show that this set $\mathbf{A}$ will be UDA for any pure state, we look at the traceless Hermitian operator $H \in (\text{span}(\mathbf{A}))^{\perp}$, where

$$\begin{aligned}H = &\alpha_1 IXZ + \alpha_2 IYZ + \alpha_3 IZX + \alpha_4 IZY + \alpha_5 IZZ\\ &+ \alpha_6 XII + \alpha_7 XIX + \alpha_8 XIY + \alpha_9 XXI\\ &+ \alpha_{10} XXZ + \alpha_{11} XYI + \alpha_{12} XYZ + \alpha_{13} XZI\\ &+ \alpha_{14} XZZ + \alpha_{15} YII + \alpha_{16} YIX + \alpha_{17} YIY\\ &+ \alpha_{18} YIZ + \alpha_{19} YXI + \alpha_{20} YYI + \alpha_{21} YZX\\ &+ \alpha_{22} YZY + \alpha_{23} YZZ + \alpha_{24} ZIX + \alpha_{25} ZIY\\ &+ \alpha_{26} ZIZ + \alpha_{27} ZXI + \alpha_{28} ZXX + \alpha_{29} ZXY\\ &+ \alpha_{30} ZYI + \alpha_{31} ZYX + \alpha_{32} ZYY + \alpha_{33} ZZI.\end{aligned}$$

It can be shown that H either has at least two positive and two negative eigenvalues or $H = 0$ (see the Appendices for details). Therefore, set $\mathbf{A}$ and any set which is Clifford equivalent to it are our optimum Pauli measurement sets for three-qubit pure-state tomography.

III. STABILITY OF THE PROTOCOL AGAINST DEPOLARIZING NOISE

Before we test our protocol experimentally, we would like to understand how robust it is given states that are not pure. Due to noise in the implementation, we often end up with some mixed state which is close to our ideal pure state. Therefore, for the protocol to work in practice, one requires it to return a density matrix with high fidelity with respect to our input state when it has high purity.

We generate a random pure state $|\phi\rangle$ from the Haar measure as our desired ideal state, then run it through a depolarizing channel to get a noisy mixed state $\rho = \eta \frac{I}{d} + (1-\eta)|\phi\rangle\langle\phi|$. We could then generate all Pauli measurement results $\{\text{Tr}(\rho\sigma_k) = M_k\}$, where σ_k is Pauli observable of given dimension. Picking results determined by our optimum Pauli measurement set as given in Eq. (6), we run a maximum likelihood estimation to get a density matrix reconstruction.

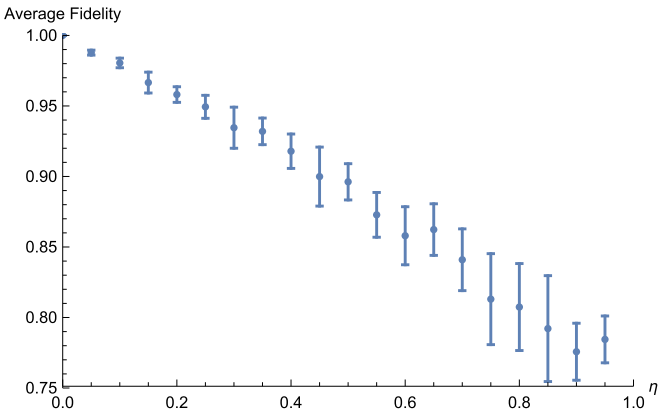

FIG. 1. Average fidelity of reconstructed density matrices compared to the ideal state using an optimum Pauli measurement set for 3 qubits. The error bars are given by standard deviation of the said fidelity over 100 instances. For small noise η, the state is very close to pure, and the protocol returns a high-fidelity density-matrix reconstruction. As noise η increases, the pure-state assumption becomes less useful, which yields a low-fidelity estimation.

If we assume the reconstructed state is low rank and η is very close to zero, the robustness of said reconstruction was shown in [14]. In our simulation, we made no assumption of the reconstructed state other than the requirement of it being semipositive definite and trace one.

For each given noise η, we take 100 different input state and run our protocol to get 100 reconstructed density matrices. The reconstructed matrices are compared to the input state to get fidelity of the reconstruction. We then take the average of these 100 fidelity and report an average fidelity for the given noise η. Our protocol is tested over a range of different η, and the results are shown in Fig. 1. We can see that for small noise η, the simulated state is very close to pure, and the protocol returns a high-fidelity density-matrix reconstruction. As noise η increases, the pure-state assumption becomes less useful, and our protocol yields a low-fidelity estimation.

IV. EXPERIMENTS IN NMR SYSTEMS

A nuclear magnetic resonance (NMR) system is an ideal testbed for our protocol. However, the creation of a pure state in NMR requires unrealistic experimental conditions such as extremely low temperatures or high magnetic fields, which makes it impractical for a liquid sample. To overcome this problem, one can prepare a pseudopure state (PPS) alternatively

$$\rho_{\text{PPS}} = \frac{1-\epsilon}{2^N}\mathbb{I} + \epsilon|\phi\rangle\langle\phi|, \tag{7}$$

where $\mathbb{I}$ is the identity matrix and $\epsilon \sim 10^{-5}$ represents the polarization. For a traceless Pauli observable σ, only the pure-state portion $\epsilon|\phi\rangle\langle\phi|$ contributes to the measurement result. Therefore, the behavior of a system in the PPS is exactly the same as it would be in the pure state.

(a)

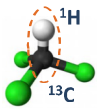

	^{1}H	^{13}C	T_1 (s)	T_2 (s)
^{1}H	500M		4.8	3.3
^{13}C	214.6	125M	17.2	0.35

(b)

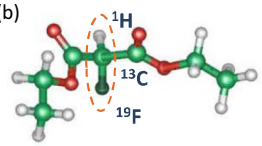

	^{1}H	^{13}C	^{19}F	T_1 (s)	T_2 (s)
^{1}H	400M			2.8	1.2
^{13}C	160.7	100M		2.9	1.1
^{19}F	47.6	-194.4	376M	3.1	1.3

FIG. 2. Molecular structure of (a) two-qubit sample ^{13} C-labeled chloroform and (b) three-qubit sample diethyl-fluoromalonate. The corresponding tables on the right side summarize the relevant NMR parameters at room temperature, including the Larmor frequencies (diagonal, in hertz), the J-coupling constant (off-diagonal, in hertz), and the relaxation time scales T_1 and T_2.

To test our protocol, we carried out the experiments in two- and three-qubit NMR quantum systems, respectively. The qubits in the two-qubit system are denoted by the ^{13}C and ^{1}H spins of ^{13}C-labeled chloroform diluted in acetone-d6 on a Bruker DRX-500 MHz spectrometer, and in the three-qubit system by the ^{13}C, ^{1}H, and ^{19}F spins in diethyl-fluoromalonate dissolved in d-chloroform on a Bruker DRX-400 MHz spectrometer. The molecular structures and relevant parameters are shown in Fig. 2, and the corresponding natural Hamiltonian for each system can be described as

$$\mathcal{H}_{\text{int}} = \sum_{i=1} \pi \nu_i \sigma_z^i + \sum_{i<j,=1} \frac{\pi J_{ij}}{2} \sigma_z^i \sigma_z^j, \tag{8}$$

where ν_i is the resonance frequency of spin i and J_{ij} are the scalar coupling constants between spins i and j. All parameters are listed in the right table of Fig. 2. Note that in experiment we set $\nu_i = 0$ in the multirotating frame for simplicity.

In experiment, the entire tomography process for a PPS becomes: given measurements $\text{Tr}(\rho\sigma_k) = \epsilon \text{Tr}(\rho_t \sigma_k) = M_k$, find a density matrix ρ_{rec} to best fit the data M_k. In order to evaluate the performance of our protocol, two comparisons will be made. First, we compare the reconstructed state using the optimum number of Pauli measurements with the one obtained with full tomography. It gives us an idea how good the reconstruction is, and whether the protocol works. Second, we compare our result with the state reconstructed by randomly choosing Pauli measurements. This tells us how different the performance is between selecting the optimum set and a random set of Pauli measurements.

A. Pure-state tomography for a two-qubit state

For the two-qubit protocol, the system is first initialized to the PPS

$$\rho_{00} = \frac{1-\epsilon}{4} \mathbb{I} + \epsilon |00\rangle\langle 00| \tag{9}$$

via spatial average technique [21,22], where $\mathbb{I}$ is the 4×4 identity and $\epsilon \sim 10^{-5}$ the polarization. The NMR signal of this PPS is used as references for further comparisons with the tomographic results. We then turn on the transversal field with the strength ω_x (in terms of radius), so the Hamiltonian

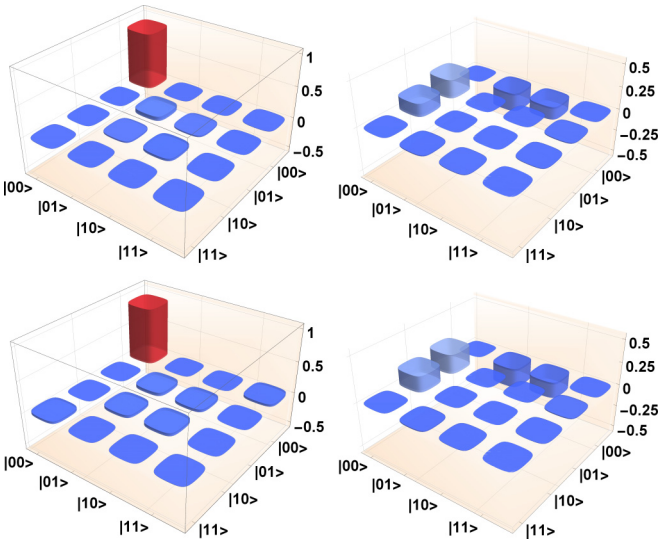

FIG. 3. Reconstruction of density matrix for state number one. The upper two figures are real and imaginary part of density matrix of state reconstruction using all 16 Pauli measurements. The bottom two figures are real and imaginary part of density matrix of state reconstruction using 11 optimum Pauli measurements described earlier. The fidelity between the two density matrices is 0.992.

becomes

$$\mathcal{H} = \frac{\omega_x}{2}(\sigma_x^1 + \sigma_x^2) + \frac{\omega_z}{2}(\sigma_z^1 + \sigma_z^2) + \pi \frac{J_{12}}{2} \sigma_z^1 \sigma_z^2. \tag{10}$$

By ignoring the identity in ρ_{00}, the system should evolve to a time-dependent pure state

$$|\phi\rangle = \alpha(t)|00\rangle + \beta(t)(|01\rangle + |10\rangle)/\sqrt{2} + \gamma(t)|11\rangle, \tag{11}$$

where t is the evolution time and $\alpha(t), \beta(t)$ $\gamma(t)$ could be calculated using the Hamiltonian in Eq. (10) (for details see Eq. (4) in [23]). We measured in total 16 different states at a few different time steps using Pauli observables. The measurement result at each time step is used as one instance of the input to our tomography algorithm. We then adopted the maximum likelihood method to reconstruct the states. The reconstructed density matrices for the first and sixteenth experiments are shown in Fig. 3. Note that as the time progresses, the relaxation becomes more prominent, where the purity of state $\text{Tr}(\rho^2)$ drops. Since our protocol is designed for pure-state tomography, the performance of our protocol is expected to drop along with the decrease of purity in a quantum state. The fidelity of different reconstructions compare to the state intended to prepare also drops (see Appendix B for detail), but it is irrelevent for the purpose of comparing two tomography methods.

In order to further demonstrate the advantages of our protocol, we compare it to a quantum state tomography with Pauli measurements. Using the same number of random Pauli measurements, one could also perform the maximum likelihood method to get a reconstruction of the density matrix. Note that the optimum set of 11 Pauli measurements may be randomly hit in this case, which means the best performance of random Pauli measurement algorithm is the same compared with our protocol. However, in a realistic setting, only one set

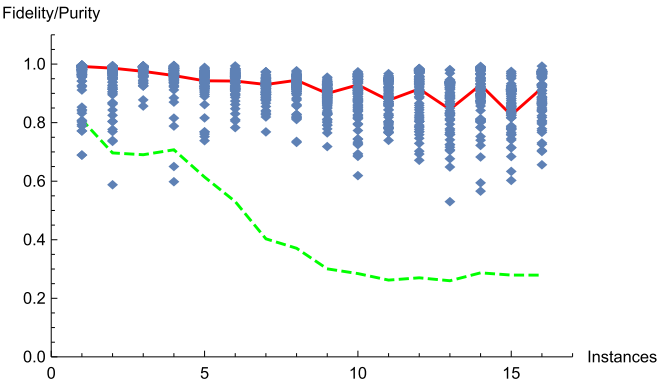

FIG. 4. Performance of two-qubit protocol using selected Pauli measurements against randomly Pauli measurements.The blue diamond dots are the fidelity between density matrix reconstructed from all 16 Pauli measurements with density matrix reconstructed from random 11 Pauli measurements. The red line represents fidelity of reconstruction using our protocol, and the green dashed line shows the purity of density matrix reconstructed from all Pauli measurements.

of random Pauli measurements will be chosen. To show the advantage of our protocol, we only have to outperform the average case of this random algorithm.

We randomly generated 11 distinct two-qubit Pauli measurements (including identity), and used the maximum likelihood method to get an estimate of our density matrix. If the density matrix given by this set of measurements is not unique, the maximum likelihood method runs multiple times to get an average estimation. For each experiment, 100 sets of random Pauli measurements were chosen. The result is shown in Fig. 4. We can see that for high purity, our method significantly outperforms the random Pauli algorithm. The advantage decreases as purity decreases, which indicates our method is more efficient for a state that is close to pure.

B. Pure-state tomography for a three-qubit state

For three-qubit system, we are interested in the GHZ state $|\mathrm{GHZ}\rangle = (|000\rangle + |111\rangle)/\sqrt{2}$. The experimental data is from [24], and the GHZ state is prepared via global controls in closed linear Ising spin chains with nearest-neighbor couplings as shown in Fig. 5. We measured all 64 Pauli measurements (the measured purity of the prepared state is about 0.89), and only use 31 of them described in Eq. (6) for our protocol. As shown in Fig. 6, only using less than half of the desired measurements, we reconstructed density matrices for the GHZ state via the maximum likelihood method with 0.96 fidelity. We then compare it to a quantum state tomography algorithm implementing 31 random Pauli measurements (including identity). Since the number of unused Pauli measurements are much more compared to the two-qubit case, we are less likely to hit the optimum set in this random algorithm. By implementing a similar maximum likelihood reconstruction, we found the average fidelity of this random algorithm to be 0.87 with standard deviation of 0.16. The detailed result is shown in Fig. 7, which shows clearly that our protocol has a decent advantage over the average case in the randomized algorithm.

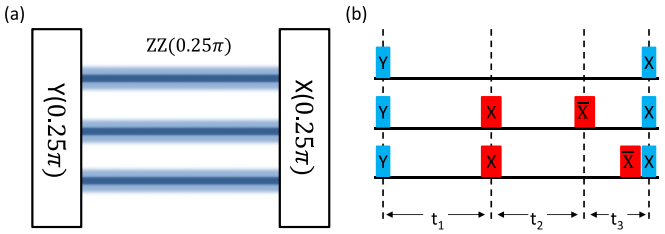

FIG. 5. (a) General scheme to create the GHZ state via global controls. $\mathrm{X}(\theta)$ and $\mathrm{Y}(\theta)$ are, respectively, the global rotations with θ angle along x and y directions, and $\mathrm{ZZ}(\tau)$ denotes a free evolution with the τ time under the model Ising Hamiltonian. (b) NMR sequence to realize the GHZ state creation from the PPS. Blue and red rectangles represent $\pi/2$ and π rotations, respectively. The evolution times are $t_1 = 6.76$ ms, $t_2 = 6.49$ ms, and $t_3 = 2.84$ ms with our sample.

V. APPLICATION TO TOMOGRAPHY IN OPTICAL SYSTEMS

Figure 8 depicts a typical scheme for measuring a polarization-encoded n-photon state [25–30]. Quarter- and half-waveplates in each photon's path are rotated to choose a separable polarization basis. We call the set of angles specifying each waveplate's position the *setting* of the measurement. The n-photon state is projected onto the basis set by the waveplate angles with n polarizing beamsplitters. A single-photon detector is present in each of the $2n$ output ports of the beamsplitters, and n-fold coincident detections among the n paths are counted. There are 2^n combinations of n-fold coincident detection events that correspond to a state with one photon entering each of the n beamsplitters before being detected in one of the two output ports. Summing the total number of n-fold coincidences over these 2^n combinations

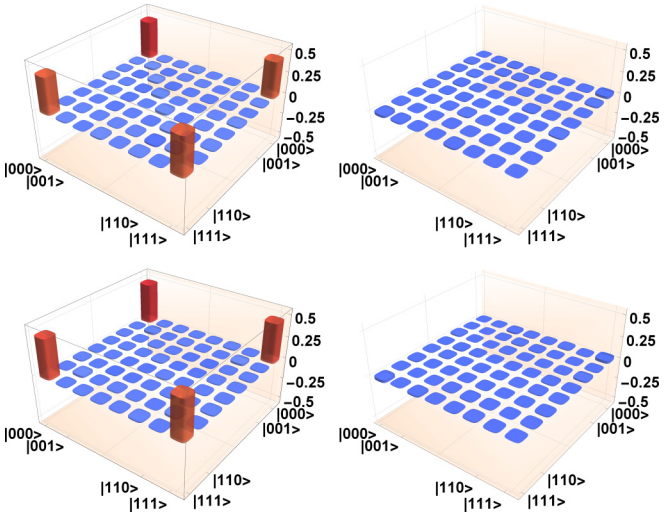

FIG. 6. Reconstruction of density matrix for GHZ state. The upper two figures are real and imaginary part of density matrix of state reconstruction using all 64 Pauli measurements. The bottom two figures are real and imaginary part of density matrix of state reconstruction using 31 optimum Pauli measurements described in Eq. (6). The fidelity between the two density matrices is 0.960.

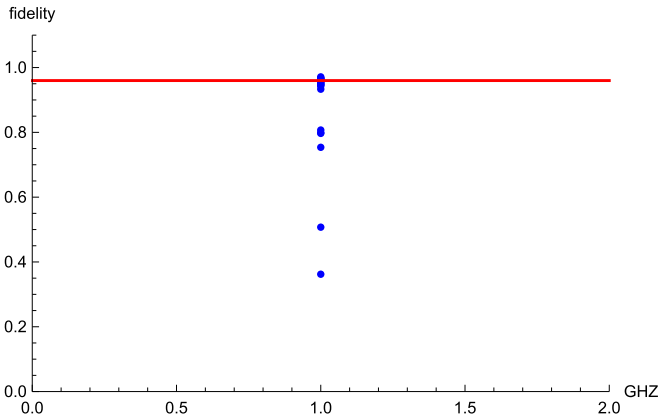

FIG. 7. Performance of three-qubit protocol using selected Pauli measurements against randomly Pauli measurements. Blue dots represent fidelity between density matrix reconstructed from all 64 Pauli measurements and density matrix reconstructed from random 31 Pauli measurements. The red square represents fidelity of reconstruction using our protocol.

gives the total number of copies of the state detected by the measurement.

A minimum of 3^n measurement settings are required for general state tomography using separable projective measurements [2]. We note that, if one performs nonseparable measurements, then general state tomography can be performed with $2^n + 1$ measurement settings [31]. However, these types of measurements are difficult to perform in practice, so we restrict the discussion here to separable ones.

One can think of each setting as a projective measurement that produces results for multiple Pauli operators simultaneously. For example, consider measuring a two-photon state with the waveplates set such that a photon in the positive eigenstate of the Pauli X or Y operator will be deterministically

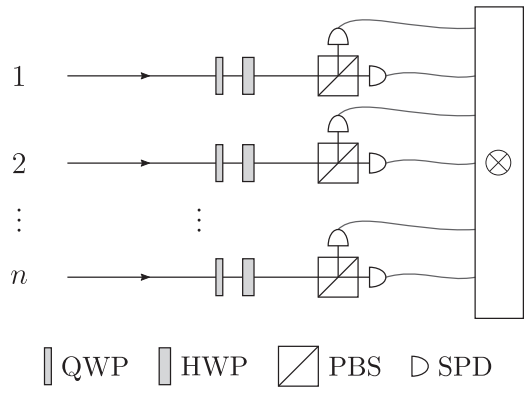

FIG. 8. Measurement scheme for a polarization-encoded n-photon state. The n-qubit state is encoded in the polarizations of the n photons. Each photon is measured using a quarter-waveplate (QWP), half-waveplate (HWP), and a polarizing beamsplitter (PBS) with a single-photon counting detector (SPD) at each of its output ports. The quarter- and half-waveplates are rotated to choose the measurement basis for each photon. Separable projective measurements are performed by counting coincident detection events between all n photons.

transmitted at the first or second beamsplitter, respectively. For simplicity we will call this the XY setting. There are four relevant twofold coincident detection events, which we denote N_{tt}, N_{tr}, N_{rt}, and N_{rr}, and where the first and second subscripts represent which output port (i.e., transmitted or reflected) the first or second photon was detected, respectively. These counts can be summed in specific ways to find expectation values of different Pauli operators. For example, the expectation value of $\langle XY\rangle$ is given by $\langle XY\rangle = (N_{tt} - N_{tr} - N_{rt} + N_{rr})/N$, where the total number of copies N is given by $N = N_{tt} + N_{tr} + N_{rt} + N_{rr}$. Similarly, $\langle XI\rangle$ can be found with $\langle XI\rangle = (N_{tt} + N_{tr} - N_{rt} - N_{rr})/N$. In total, the XY setting measures the following four Pauli operators:

$$XY, XI, IY, II.$$

Based on this observation, we can use the results of Theorem 1 and Theorem 2 to reduce the number of settings to UDA pure states. For the two-qubit case, recall that the 11 Pauli operators to UDA any pure states are

$$A = \{II, IX, IY, IZ, XI, YX, YY, YZ, ZX, ZY, ZZ\}.$$

Notice that any of the six Paulis with no I component (the two-qubit correlations) only appear in the setting which measures it. However, looking at the remaining five Paulis, II is included in every setting, IX is included in the YX setting, IY in YY, and IZ in YZ. The only operator which does not appear in the settings of the two-qubit correlations is XI, so for the two-qubit case, $6 + 1 = 7$ settings are required to be sufficient for UDA.

And similar analysis can be done for the three-qubit case, with the aid of computer search. That is, we find the minimum number of settings that can produce all the 31 Pauli operators as given in Eq. (6). We summarize these results as the corollary below.

Corollary 1: Only seven settings

$$\{XI, YX, YY, YZ, ZX, ZY, ZZ\}.$$

are needed to UDA any two-qubit pure states, compared with nine settings needed for general two-qubit state tomography. And only 19 settings

$$\begin{aligned}\{&XXZ, XYZ, XZX, XZY, XZZ, YXX,\\ &YXY, YYX, YYY, YZX, YZY, YZZ,\\ &ZXX, ZXY, ZXZ, ZYX, ZYY, ZYZ, ZZX\}\end{aligned} \quad (12)$$

are needed to UDA any three-qubit pure states, compared with 27 settings needed for general three-qubit state tomography.

We remark that Corollary 1 is a direct application of Theorem 1 and Theorem 2. It is possible for even better results to be obtained by including knowledge of settings in the first optimization. However, proving sufficiency becomes more difficult in these cases.

VI. CONCLUSION

In this work, we find the most compact Pauli measurement sets for pure-state tomography on two- and three-qubit systems. The experiments on two-qubit and three-qubit NMR systems demonstrated the advantages of using such protocol. We reduced the required number of measurements by five

and 33 for two- and three-qubit systems, respectively, without significant drop in fidelity. As a direct application of this result, we also showed that our scheme can be used to reduce the number of settings needed for pure-state tomography in quantum optics systems.

A few questions need to be answered before we scale the test to larger systems. We are able to find the optimum sets for two and three qubits. However, the method we used to find those sets cannot be easily generalized to larger systems. It remains open whether one can find a general algorithm to decide the smallest sets of Pauli operators to UDA any pure state for a system of n qubits. If such an algorithm exists, we would hope that the number of measurements required grows linearly with the Hilbert space dimension of the system.

ACKNOWLEDGMENTS

We thank Nengkun Yu for helpful discussions. This research was supported in part by the Natural Sciences and Engineering Research Council of Canada (NSERC), Canada Research Chairs, Industry Canada, National Key Basic Research Program (Grants No. 2013CB921800 and No. 2014CB848700), the National Science Fund for Distinguished Young Scholars (Grant No. 11425523), and National Natural Science Foundation of China (Grant No. 11375167).

APPENDIX A: PROOF OF THEOREM 2

In order to prove Theorem 2, it suffices to prove the following result.

Theorem 3. Any Hermitian operator perpendicular to

$$\begin{aligned}\{&IIX, IIY, IIZ, IXI, IXX, IXY, IYI, IYX, IYY, IZI,\\ &XIZ, XXX, XXY, XYX, XYY, XZX, XZY, YXX,\\ &YXY, YXZ, YYX, YYY, YYZ, YZI, ZII, ZXZ, ZYZ,\\ &ZZX, ZZY, ZZZ\}\end{aligned}$$

must have at least two positive and two negative eigenvalues.

Proof. The proof proceeds as follows. First construct an 8×8 traceless Hermitian matrix H which is perpendicular to all the above Pauli operators. This will be a real linear combination of every Pauli operator that is not being measured. This H is then a general description of any Hermitian matrix in the complement of the span of all measured operators. We will show through a case by case analysis that if we assume H only has one positive eigenvalue, then it follows that H must be the zero matrix. A similar argument holds for having only one negative eigenvalue; therefore, H must have at least two positive and two negative eigenvalues.

Let us begin by constructing H which is a real linear combination of the 33 Pauli operators not being measured (excluding the identity). H is then

$$\begin{aligned}H = {}& x_1 IXZ + x_2 IYZ + x_3 IZX + x_4 IZY\\ &+ x_5 IZZ + x_6 XII + x_7 XIX + x_8 XIY\\ &+ x_9 XXI + x_{10} XXZ + x_{11} XYI + x_{12} XYZ\\ &+ x_{13} XZI + x_{14} XZZ + x_{15} YII + x_{16} YIX\\ &+ x_{17} YIY + x_{18} YIZ + x_{19} YXI + x_{20} YYI\\ &+ x_{21} YZX + x_{22} YZY + x_{23} YZZ + x_{24} ZIX\\ &+ x_{25} ZIY + x_{26} ZIZ + x_{27} ZXI + x_{28} ZXX\\ &+ x_{29} ZXY + x_{30} ZYI + x_{31} ZYX + x_{32} ZYY\\ &+ x_{33} ZZI.\end{aligned}$$

Writing H in matrix form will give the form

$$\begin{bmatrix} c_{11} & c_{12} & c_{13} & c_{14} & c_{15} & c_{16} & c_{17} & 0 \\ c_{12}^* & c_{22} & c_{23} & c_{24} & c_{25} & c_{26} & 0 & c_{28} \\ c_{13}^* & c_{23}^* & c_{33} & c_{34} & c_{35} & 0 & c_{37} & c_{38} \\ c_{14}^* & c_{24}^* & c_{34}^* & c_{44} & 0 & c_{46} & c_{47} & c_{48} \\ c_{15}^* & c_{25}^* & c_{35}^* & 0 & c_{55} & c_{56} & c_{57} & c_{58} \\ c_{16}^* & c_{26}^* & 0 & c_{46}^* & c_{56}^* & c_{66} & c_{67} & c_{68} \\ c_{17}^* & 0 & c_{37}^* & c_{47}^* & c_{57}^* & c_{67}^* & c_{77} & c_{78} \\ 0 & c_{28}^* & c_{38}^* & c_{48}^* & c_{58}^* & c_{68}^* & c_{78}^* & c_{88} \end{bmatrix}, \quad \text{(A1)}$$

where

$$\begin{aligned}c_{11} &= x_5 + x_{26} + x_{33},\\ c_{22} &= -x_5 - x_{26} + x_{33},\\ c_{33} &= -x_5 + x_{26} - x_{33},\\ c_{44} &= x_5 - x_{26} - x_{33},\\ c_{55} &= x_5 - x_{26} - x_{33} = c_{44},\\ c_{66} &= -x_5 + x_{26} - x_{33} = c_{33},\\ c_{77} &= -x_5 - x_{26} + x_{33} = c_{22},\\ c_{88} &= x_5 + x_{26} + x_{33} = c_{11},\\ c_{12} &= x_3 + x_{24} - i(x_4 + x_{25}),\\ c_{34} &= -x_3 + x_{24} + i(x_4 - x_{25}),\\ c_{56} &= x_3 - x_{24} - i(x_4 - x_{25}) = -c_{34},\\ c_{78} &= -x_3 - x_{24} + i(x_4 + x_{25}) = -c_{12},\\ c_{13} &= x_1 + x_{27} - i(x_2 + x_{30}),\\ c_{24} &= -x_1 + x_{27} + i(x_2 - x_{30}),\\ c_{57} &= x_1 - x_{27} - i(x_2 - x_{30}) = -c_{24},\\ c_{68} &= -x_1 - x_{27} + i(x_2 + x_{30}) = -c_{13},\\ c_{14} &= x_{28} - x_{32} - i(x_{29} + x_{31}),\\ c_{23} &= x_{28} + x_{32} + i(x_{29} - x_{31}),\\ c_{58} &= -x_{28} + x_{32} + i(x_{29} + x_{31}) = -c_{14},\\ c_{67} &= -x_{28} - x_{32} - i(x_{29} - x_{31}) = -c_{23},\\ c_{15} &= x_6 + x_{13} + x_{14} - i(x_{15} + x_{18} + x_{23}),\\ c_{26} &= x_6 + x_{13} - x_{14} - i(x_{15} - x_{18} - x_{23}),\\ c_{37} &= x_6 - x_{13} - x_{14} - i(x_{15} + x_{18} - x_{23}),\\ c_{48} &= x_6 - x_{13} + x_{14} - i(x_{15} - x_{18} + x_{23})\\ &= c_{15} - c_{26}^* + c_{37}^*,\\ c_{16} &= x_7 - x_{17} - x_{22} - i(x_8 + x_{16} + x_{21}),\\ c_{25} &= x_7 + x_{17} + x_{22} + i(x_8 - x_{16} - x_{21}),\\ c_{38} &= x_7 - x_{17} + x_{22} - i(x_8 + x_{16} - x_{21}),\\ c_{47} &= x_7 + x_{17} - x_{22} + i(x_8 - x_{16} + x_{21})\\ &= c_{16}^* + c_{25} - c_{38}^*,\end{aligned}$$

$$
\begin{aligned}
c_{17} &= x_9 + x_{10} - x_{20} - i(x_{11} + x_{12} + x_{19}),\\
c_{28} &= x_9 - x_{10} - x_{20} - i(x_{11} - x_{12} + x_{19}),\\
c_{35} &= x_9 + x_{10} + x_{20} + i(x_{11} + x_{12} - x_{19}),\\
c_{46} &= x_9 - x_{10} + x_{20} + i(x_{11} - x_{12} - x_{19})\\
&= c_{28}^* + c_{35} - c_{17}^*.
\end{aligned}
$$

Note that the main antidiagonal is all zeros. This was by design, since any set of Pauli operators Clifford equivalent to the result from the hypergraph dualization program is also a solution, we had the freedom to choose a set which would make the proof simpler. Choosing the set of operators which contained all Pauli operators constructed by tensoring only X operators and Y operators meant H would have zero main antidiagonal. The only reason for choosing this set is it makes this proof a little simpler.

Here we assume H is a Hermitian matrix with only one positive eigenvalue. We first show all diagonal entries of H must be zero. Observe that $c_{55} = c_{44}$, $c_{66} = c_{33}$, $c_{77} = c_{22}$, and $c_{88} = c_{11}$. In order for the traceless condition on H to hold, it is then clear that $c_{11} + c_{22} + c_{33} + c_{44} = 0$. If H has some nonzero diagonal entry, then at least one of c_{11}, c_{22}, c_{33}, and c_{44} will be positive. Without loss of generality, let $c_{11} > 0$, then the submatrix of H formed by the rows $(1,8)$ and columns $(1,8)$, which will be of the form $c_{11} * I$, will have two positive eigenvalues.

Lemma 1. Cauchy's Interlacing Theorem states [32] the following. Let

$$
A = \begin{bmatrix} B & C \\ C^\dagger & D \end{bmatrix}
$$

be an $n \times n$ Hermitian matrix, where B has size $m \times m$ ($m < n$). If the eigenvalues of A and B are $\alpha_1 \leqslant \cdots \leqslant \alpha_n$ and $\beta_1 \leqslant \cdots \leqslant \beta_m$ respectfully. Then

$$
\alpha_k \leqslant \beta_k \leqslant \alpha_{k+n-m}, k = 1, \ldots, m.
$$

It follows from Cauchy's interlacing property that if a principle submatrix of H has two positive eigenvalues then H also has at least two positive eigenvalues.

Hence H must be in the following form:

$$
H = \begin{bmatrix}
0 & c_{12} & c_{13} & c_{14} & c_{15} & c_{16} & c_{17} & 0 \\
c_{12}^* & 0 & c_{23} & c_{24} & c_{25} & c_{26} & 0 & c_{28} \\
c_{13}^* & c_{23}^* & 0 & c_{34} & c_{35} & 0 & c_{37} & c_{38} \\
c_{14}^* & c_{24}^* & c_{34}^* & 0 & 0 & c_{28}^* + c_{35} - c_{17}^* & c_{16}^* + c_{25} - c_{38}^* & c_{15} - c_{26}^* + c_{37}^* \\
c_{15}^* & c_{25}^* & c_{35}^* & 0 & 0 & -c_{34} & -c_{24} & -c_{14} \\
c_{16}^* & c_{26}^* & 0 & c_{28} + c_{35}^* - c_{17} & -c_{34}^* & 0 & -c_{23} & -c_{13} \\
c_{17}^* & 0 & c_{37}^* & c_{16} + c_{25}^* - c_{38} & -c_{24}^* & -c_{23}^* & 0 & -c_{12} \\
0 & c_{28}^* & c_{38}^* & c_{15}^* - c_{26} + c_{37} & -c_{14}^* & -c_{13}^* & -c_{12}^* & 0
\end{bmatrix}.
$$

In fact, under the assumption that H has only one positive eigenvalue, it follows from Cauchy's interlacing theorem that any principle submatrix of H cannot have more than one positive eigenvalue. Otherwise, we will have a contradiction.

Let us look at the submatrix formed by rows $1,2,4,5$ and the same columns. It is a traceless Hermitian matrix with determinant $|c_{14}c_{25} - c_{15}c_{24}|^2$. Again, if the submatrix has positive determinant, then it must have exactly two positive eigenvalues. Once again by applying Cauchy's interlacing property, H will have at least two positive eigenvalues. This immediately contradicts our assumption. The above argument implies that, under our assumption H has only one positive eigenvalue, we have $|c_{14}c_{25} - c_{15}c_{24}|^2 \leqslant 0$. It is not surprising that the inequality holds if and only if the equality holds. Then we have $c_{14}c_{25} - c_{15}c_{24} = 0$.

Similarly, by considering other 4×4 submatrices constructed from the rows and columns $a,b,4,5$, where a,b are any two of the remain six rows, we can show that

$$
\begin{aligned}
c_{14}c_{35} - c_{15}c_{34} &= 0,\\
-c_{14}c_{34}^* - c_{15}(c_{28} + c_{35}^* - c_{17}) &= 0,\\
-c_{14}c_{24}^* - c_{15}(c_{16} + c_{25}^* - c_{38}) &= 0,\\
-c_{14}c_{14}^* - c_{15}(c_{15}^* - c_{26} + c_{37}) &= 0,\\
c_{24}c_{35} - c_{25}c_{34} &= 0,\\
-c_{24}c_{34}^* - c_{25}(c_{28} + c_{35}^* - c_{17}) &= 0,\\
-c_{24}c_{24}^* - c_{25}(c_{16} + c_{25}^* - c_{38}) &= 0,\\
-c_{24}c_{14}^* - c_{25}(c_{15}^* - c_{26} + c_{37}) &= 0,\\
-c_{34}c_{34}^* - c_{35}(c_{28} + c_{35}^* - c_{17}) &= 0,\\
-c_{34}c_{24}^* - c_{35}(c_{16} + c_{25}^* - c_{38}) &= 0,\\
-c_{34}c_{14}^* - c_{35}(c_{15}^* - c_{26} + c_{37}) &= 0,\\
-c_{24}^*(c_{28} + c_{35}^* - c_{17}) + c_{34}^*(c_{16} + c_{25}^* - c_{38}) &= 0,\\
-c_{14}^*(c_{28} + c_{35}^* - c_{17}) + c_{34}^*(c_{15}^* - c_{26} + c_{37}) &= 0,\\
-c_{14}^*(c_{16} + c_{25}^* - c_{38}) + c_{24}^*(c_{15}^* - c_{26} + c_{37}) &= 0.
\end{aligned}
$$

The above equations will imply that the 8×2 submatrix formed by the fourth and fifth columns has rank at most 1. The same argument can be used to prove that the 8×2 submatrices formed by columns (1,8), (2,7), or (3,6) also have rank at most 1.

As a straightforward consequence, H has rank no more than 4.

In other words, the kth column and the $(9-k)$th column are linearly dependent. This means that there exist $\lambda_1,\lambda_2,\lambda_3,\lambda_4$ such that the following equations hold:

$$\lambda_1\overrightarrow{C_1} + (1-\lambda_1)\overrightarrow{C_8} = \lambda_2\overrightarrow{C_2} + (1-\lambda_2)\overrightarrow{C_7} = 0, \tag{A2}$$

$$\lambda_3\overrightarrow{C_3} + (1-\lambda_3)\overrightarrow{C_6} = \lambda_4\overrightarrow{C_4} + (1-\lambda_4)\overrightarrow{C_5} = 0. \tag{A3}$$

Here we have used $\overrightarrow{C_k}$ to represent the kth column of the matrix (A2).

Let us start with a special case. Let $\lambda_1 = 0$. Then $c_{12} = c_{13} = c_{14} = c_{28} = c_{38} = 0$ and $c_{15} = c_{26}^* - c_{37}^*$. H can be simplified as the following:

$$H = \begin{bmatrix} 0 & 0 & 0 & 0 & c_{26}^* - c_{37}^* & c_{16} & c_{17} & 0 \\ 0 & 0 & c_{23} & c_{24} & c_{25} & c_{26} & 0 & 0 \\ 0 & c_{23}^* & 0 & c_{34} & c_{35} & 0 & c_{37} & 0 \\ 0 & c_{24}^* & c_{34}^* & 0 & 0 & c_{35} - c_{17}^* & c_{16}^* + c_{25} & 0 \\ c_{26} - c_{37} & c_{25}^* & c_{35}^* & 0 & 0 & -c_{34} & -c_{24} & 0 \\ c_{16}^* & c_{26}^* & 0 & c_{35}^* - c_{17} & -c_{34}^* & 0 & -c_{23} & 0 \\ c_{17}^* & 0 & c_{37}^* & c_{16} + c_{25}^* & -c_{24}^* & -c_{23}^* & 0 & 0 \\ 0 & 0 & 0 & 0 & 0 & 0 & 0 & 0 \end{bmatrix}.$$

If we set $c_{23} = c_{24} = c_{34} = 0$, then the top-left 4×4 submatrix is zero. In this case, the characteristic polynomial of H contains only even powers. Thus H having only one positive eigenvalue implies H has only one negative eigenvalue too. As a consequence, the top-right 4×4 submatrix of H has rank exactly 1.

As a result, any 2×2 submatrix of the top-right submatrix must have determinant zero. From suitable choices of submatrices we can obtain the following equations:

$$c_{26}c_{37} = 0, \tag{A4}$$

$$c_{26}(c_{26}^* - c_{37}^*) = c_{16}c_{25}, \tag{A5}$$

$$c_{37}(c_{26}^* - c_{37}^*) = c_{17}c_{35}, \tag{A6}$$

$$c_{16}(c_{16}^* + c_{25}) + c_{17}(c_{17}^* - c_{35}) = 0. \tag{A7}$$

Using the above equations we can obtain

$$\begin{aligned} 0 &= c_{16}(c_{16}^* + c_{25}) + c_{17}(c_{17}^* - c_{35}) \\ &= c_{16}c_{25} - c_{17}c_{35} + |c_{17}|^2 + |c_{16}|^2 \\ &= c_{26}(c_{26}^* - c_{37}^*) - c_{37}(c_{26}^* - c_{37}^*) + |c_{17}|^2 + |c_{16}|^2 \\ &= |c_{26} - c_{37}|^2 + |c_{17}|^2 + |c_{16}|^2. \end{aligned} \tag{A8}$$

This implies $c_{16} = c_{17} = 0$ and $c_{26} = c_{37}$. Also since $c_{26}c_{37} = 0$ we know that $c_{26} = c_{37} = 0$. Furthermore $c_{25}(c_{16}^* + c_{25}) = 0$ and $c_{35}(c_{35} - c_{17}^*) = 0$ will guarantee $c_{25} = c_{35} = 0$. Therefore H is once again the zero matrix.

We must then assume at least one of c_{23},c_{24},c_{34} must be nonzero. If $c_{23} \neq 0$, then by considering submatrices formed by rows or columns $(1,2,3,k)$ $(5 \leqslant k \leqslant 8)$, we have $c_{16} = c_{17} = 0$ and $c_{26} = c_{37}$. For the case that $c_{24} = 0$ or $c_{34} = 0$, we will also have $c_{16} = c_{17} = 0$ and $c_{26} = c_{37}$ by considering appropriately chosen submatrices.

We are then left with H in the form

$$H = \begin{bmatrix} 0 & 0 & 0 & 0 & 0 & 0 & 0 & 0 \\ 0 & 0 & c_{23} & c_{24} & c_{25} & c_{26} & 0 & 0 \\ 0 & c_{23}^* & 0 & c_{34} & c_{35} & 0 & c_{26} & 0 \\ 0 & c_{24}^* & c_{34}^* & 0 & 0 & c_{35} & c_{25} & 0 \\ 0 & c_{25}^* & c_{35}^* & 0 & 0 & -c_{34} & -c_{24} & 0 \\ 0 & c_{26}^* & 0 & c_{35}^* & -c_{34}^* & 0 & -c_{23} & 0 \\ 0 & 0 & c_{26}^* & c_{25}^* & -c_{24}^* & -c_{23}^* & 0 & 0 \\ 0 & 0 & 0 & 0 & 0 & 0 & 0 & 0 \end{bmatrix}$$

Now, recall the fact that the submatrices formed by the kth and the $(9-k)$th columns will always have rank 1. From this it can be shown we will have H is a zero matrix.

Take the submatrix formed by the second and seventh columns for example. Since they are linearly dependent, the determinant of any 2×2 submatrix must be zero. From this we can get that $|c_{23}|^2 + |c_{26}|^2 = 0$. Therefore, $c_{23} = c_{26} = 0$. By similar arguments on various submatrices, H can be shown to be the zero matrix.

Thus, under our assumption that H has exactly one positive eigenvalue, $\lambda_1 \neq 0$. Similarly, we can also prove that $\lambda_1 \neq 1,\lambda_2,\lambda_3,\lambda_4 \neq 0,1$. We can then assume from now on that H has no zero columns or rows.

Hence there exists certain $\lambda_1,\lambda_2,\lambda_3$, and $\lambda_4 \neq 0,1$ which satisfies Eq. (A2).

Let us use Re and Im to denote the real part and imaginary part of a complex number. Then the above equations can be rewritten as linear equations of real numbers.

Let us use $M(\lambda_1,\lambda_2,\lambda_3,\lambda_4)$ to denote the 48×30 coefficient matrix. If we can prove that the coefficient matrix always has rank 30 for any $\lambda_1,\lambda_2,\lambda_3$, and λ_4, then it will imply that all c_{ij}'s are zeros which will immediately contradict our assumption.

Unfortunately, we are not that lucky. $M(\lambda_1,\lambda_2,\lambda_3,\lambda_4)$ will be degenerate under certain assignment of variables $(\lambda_1,\lambda_2,\lambda_3,\lambda_4)$. For example, $\text{rank}(M(\frac{1+i}{2},\frac{1+i}{2},\frac{1+i}{2},\frac{1+i}{2})) = 27 < 30$. However, we can still show that $M(\lambda_1,\lambda_2,\lambda_3,\lambda_4)$ will have rank 30 except for some degenerate cases which will be

dealt with separately. The top-left 2×2 submatrix has rank 2 if and only if $\lambda_1 \neq 0$.

At least one of the following situations must happen.

(1) $\begin{bmatrix} -C_1 & A_1 \\ B_2 & C_2 \end{bmatrix}$ has full rank. This implies $c_{12} = c_{17} = 0$.

(2) $\begin{bmatrix} A_1 & C_1 \\ -D_2 & A_2 \end{bmatrix}$ has full rank. This implies $c_{12} = c_{28} = 0$.

(3) $\begin{bmatrix} B_3 & C_3 \\ -C_1 & A_1 \end{bmatrix}$ has full rank. This implies $c_{13} = c_{16} = 0$.

(4) $\begin{bmatrix} A_1 & C_1 \\ -D_3 & A_3 \end{bmatrix}$ has full rank. This implies $c_{13} = c_{38} = 0$.

(5) $\begin{bmatrix} -C_1 & A_1 \\ B_4 & C_4 \end{bmatrix}$ has full rank. This implies $c_{14} = c_{15} = 0$.

(6) $\begin{bmatrix} -C_2 & A_2 \\ B_3 & C_3 \end{bmatrix}$ has full rank. This implies $c_{23} = c_{26} = 0$.

(7) $\begin{bmatrix} A_2 & C_2 \\ -D_3 & A_3 \end{bmatrix}$ has full rank. This implies $c_{23} = c_{37} = 0$.

(8) $\begin{bmatrix} -C_2 & A_2 \\ B_4 & C_4 \end{bmatrix}$ has full rank. This implies $c_{24} = c_{25} = 0$.

(9) $\begin{bmatrix} -C_3 & A_3 \\ B_4 & C_4 \end{bmatrix}$ has full rank. This implies $c_{34} = c_{35} = 0$.

(10)
$$\begin{aligned} \det\left(\begin{bmatrix} -C_1 & A_1 \\ B_2 & C_2 \end{bmatrix}\right) &= \det\left(\begin{bmatrix} A_1 & C_1 \\ -D_2 & A_2 \end{bmatrix}\right) \\ &= \det\left(\begin{bmatrix} B_3 & C_3 \\ -C_1 & A_1 \end{bmatrix}\right) = \det\left(\begin{bmatrix} A_1 & C_1 \\ -D_3 & A_3 \end{bmatrix}\right) \\ &= \det\left(\begin{bmatrix} -C_1 & A_1 \\ B_4 & C_4 \end{bmatrix}\right) = \det\left(\begin{bmatrix} -C_2 & A_2 \\ B_3 & C_3 \end{bmatrix}\right) \\ &= \det\left(\begin{bmatrix} A_2 & C_2 \\ -D_3 & A_3 \end{bmatrix}\right) = \det\left(\begin{bmatrix} -C_2 & A_2 \\ B_4 & C_4 \end{bmatrix}\right) \\ &= \det\left(\begin{bmatrix} -C_3 & A_3 \\ B_4 & C_4 \end{bmatrix}\right) = 0. \end{aligned}$$

With assistance of a symbolic computation package like Mathematica, we find that the only solution to the above equations is $\mathrm{Re}\lambda_1 = \mathrm{Re}\lambda_2 = \mathrm{Re}\lambda_3 = \mathrm{Re}\lambda_4 = \frac{1}{2}$.

Here we will prove that there is no Hermitian matrix in the form (A2) with only one positive eigenvalue for every situation as follows.

(1) $c_{12} = c_{17} = 0$. Any H with only one positive eigenvalue must be in the following form:

$$H = \begin{bmatrix} 0 & 0 & c_{13} & c_{14} & c_{15} & c_{16} & 0 & 0 \\ 0 & 0 & c_{23} & c_{24} & c_{25} & c_{26} & 0 & c_{28} \\ c_{13}^* & c_{23}^* & 0 & c_{34} & c_{35} & 0 & c_{37} & c_{38} \\ c_{14}^* & c_{24}^* & c_{34}^* & 0 & 0 & c_{28}^* + c_{35} & c_{16}^* + c_{25} - c_{38}^* & c_{15} - c_{26}^* + c_{37}^* \\ c_{15}^* & c_{25}^* & c_{35}^* & 0 & 0 & -c_{34} & -c_{24} & -c_{14} \\ c_{16}^* & c_{26}^* & 0 & c_{28} + c_{35}^* & -c_{34}^* & 0 & -c_{23} & -c_{13} \\ 0 & 0 & c_{37}^* & c_{16} + c_{25}^* - c_{38} & -c_{24}^* & -c_{23}^* & 0 & 0 \\ 0 & c_{28}^* & c_{38}^* & c_{15}^* - c_{26} + c_{37} & -c_{14}^* & -c_{13}^* & 0 & 0 \end{bmatrix}.$$

By considering submatrices formed by row or columns $(1,2,p,q)$ where $3 \leqslant p < q \leqslant 8$, we have that the first two rows are linearly dependent. Under our assumption that there is no row of H containing only zero entries, we have $c_{28} = 0$.

Recall that the fourth and fifth rows are linearly dependent; thus $c_{34}(-c_{34}^*) = c_{35}(c_{28} + c_{35}^*)$ which now can be simplified as $|c_{34}|^2 + |c_{35}|^2 = 0$. Hence $c_{34} = c_{35} = 0$. Then

$$H = \begin{bmatrix} 0 & 0 & c_{13} & c_{14} & c_{15} & c_{16} & 0 & 0 \\ 0 & 0 & c_{23} & c_{24} & c_{25} & c_{26} & 0 & 0 \\ c_{13}^* & c_{23}^* & 0 & 0 & 0 & 0 & c_{37} & c_{38} \\ c_{14}^* & c_{24}^* & 0 & 0 & 0 & 0 & c_{16}^* + c_{25} - c_{38}^* & c_{15} - c_{26}^* + c_{37}^* \\ c_{15}^* & c_{25}^* & 0 & 0 & 0 & 0 & -c_{24} & -c_{14} \\ c_{16}^* & c_{26}^* & 0 & 0 & 0 & 0 & -c_{23} & -c_{13} \\ 0 & 0 & c_{37}^* & c_{16} + c_{25}^* - c_{38} & -c_{24}^* & -c_{23}^* & 0 & 0 \\ 0 & 0 & c_{38}^* & c_{15}^* - c_{26} + c_{37} & -c_{14}^* & -c_{13}^* & 0 & 0 \end{bmatrix}.$$

Again, by applying our submatrix argument, we have the submatrix formed by (3,4,5,6) columns must have rank 1.

If there is a zero element in the submatrix formed by rows (1,2,7,8) and columns (3,4,5,6), then there must be a row or a column containing only zero elements in H. So, here we assume the submatrix formed by rows (1,2,7,8) and columns (3,4,5,6) does not contain any zero element. Then $\frac{c_{15}}{c_{25}} = \frac{c_{13}}{c_{23}} = \frac{c_{38}}{c_{37}}$, which implies $c_{38}c_{25} = c_{37}c_{15}$.

Following from the rank 1 condition, we have

$$c_{15}(c_{15}^* - c_{26} + c_{37}) = -|c_{14}|^2, \quad c_{25}(c_{16} + c_{25}^* - c_{38}) = -|c_{24}|^2.$$

By substituting $c_{38}c_{25} = c_{37}c_{15}$ and $c_{15}c_{26} = c_{25}c_{16}$ into the above two equations, we have

$$\begin{aligned} |c_{15}|^2 + |c_{14}|^2 &= c_{15}c_{26} - c_{15}c_{37} \\ &= c_{25}c_{16} - c_{25}c_{38} \\ &= -|c_{24}|^2 - |c_{25}|^2, \end{aligned}$$

which implies $c_{15} = c_{14} = c_{24} = c_{25} = 0$. However, it contradicts our assumption that there is no zero element in the submatrix formed by (1,2,7,8) rows and (3,4,5,6) columns.

Similarly, we can also prove that there is no Hermitian matrix in the form (A2) with only one positive eigenvalue if any of the following conditions apply.

(2) $c_{12} = c_{28} = 0$.
(3) $c_{13} = c_{16} = 0$.
(4) $c_{13} = c_{38} = 0$.
(5) $c_{14} = c_{15} = 0$.
(6) $c_{23} = c_{26} = 0$.
(7) $c_{23} = c_{37} = 0$.
(8) $c_{24} = c_{25} = 0$.
(9) $c_{34} = c_{35} = 0$.

Now, the only case we have left is the following.

(10)$\mathrm{Re}\lambda_1 = \mathrm{Re}\lambda_2 = \mathrm{Re}\lambda_3 = \mathrm{Re}\lambda_4 = \frac{1}{2}$. In this case, $\mathrm{rank}(\begin{bmatrix} -C_1 & A_1 \\ B_2 & C_2 \end{bmatrix}) = 3$. Hence $(\mathrm{Re}c_{12}, \mathrm{Im}c_{12}, \mathrm{Re}c_{17}, \mathrm{Im}c_{17})$ lies in the null space of $\begin{bmatrix} -C_1 & A_1 \\ B_2 & C_2 \end{bmatrix} = \begin{bmatrix} -\frac{1}{2} & -b_1 & \frac{1}{2} & b_1 \\ b_1 & -\frac{1}{2} & b_1 & -\frac{1}{2} \\ \frac{1}{2} & -b_2 & \frac{1}{2} & b_2 \\ b_2 & \frac{1}{2} & -b_2 & \frac{1}{2} \end{bmatrix}$. Thus

$$[c_{12} : c_{17}] = [2(b_2 - b_1) + (1 + 4b_1b_2)i : 2(b_1 + b_2) + (4b_1b_2 - 1)i].$$

Similarly, we will have

$$\begin{aligned}
[c_{12} : c_{17} : c_{28}] &= [2(b_2 - b_1) + (1 + 4b_1b_2)i : 2(b_1 + b_2) + (4b_1b_2 - 1)i : -2(b_1 + b_2) - (4b_1b_2 - 1)i], \\
[c_{13} : c_{16} : c_{38}] &= [2(b_1 - b_3) - (1 + 4b_1b_3)i : -2(b_1 + b_3) - (4b_1b_3 - 1)i : 2(b_1 + b_3) + (4b_1b_3 - 1)i], \\
[c_{23} : c_{26} : c_{37}] &= [2(b_3 - b_2) + (4b_2b_3 + 1)i : 2(b_2 + b_3) + (4b_2b_3 - 1)i : -2(b_2 + b_3) - (4b_2b_3 - 1)i], \\
[c_{14} : c_{15}] &= [2(b_4 - b_1) - (4b_1b_4 + 1)i : 2(b_1 + b_4) + (4b_1b_4 - 1)i], \\
[c_{24} : c_{25}] &= [2(b_4 - b_2) + (4b_2b_4 + 1)i : 2(b_2 + b_4) + (4b_2b_4 - 1)i], \\
[c_{34} : c_{35}] &= [2(b_4 - b_3) + (4b_3b_4 + 1)i : 2(b_3 + b_4) + (4b_3b_4 - 1)i].
\end{aligned}$$

Here $[q_1 : q_2 : \cdots : q_m] = [r_1 + s_1 i : r_2 + s_2 i : \cdots : r_m + s_m i]$ means there exists some $\mu \in \mathbb{R}$ such that $q_i = \mu(r_i + s_i i)$ for any $1 \leqslant i \leqslant m$.

Observe that $c_{28} = -c_{17}, c_{38} = -c_{16}, c_{37} = -c_{26}$; we thus simplify the matrix form of H as the following:

$$H = \begin{bmatrix}
0 & c_{12} & c_{13} & c_{14} & c_{15} & c_{16} & c_{17} & 0 \\
c_{12}^* & 0 & c_{23} & c_{24} & c_{25} & c_{26} & 0 & -c_{17} \\
c_{13}^* & c_{23}^* & 0 & c_{34} & c_{35} & 0 & -c_{26} & -c_{16} \\
c_{14}^* & c_{24}^* & c_{34}^* & 0 & 0 & c_{35} - 2c_{17}^* & c_{25} + 2c_{16}^* & c_{15} - 2c_{26}^* \\
c_{15}^* & c_{25}^* & c_{35}^* & 0 & 0 & -c_{34} & -c_{24} & -c_{14} \\
c_{16}^* & c_{26}^* & 0 & c_{35}^* - 2c_{17} & -c_{34}^* & 0 & -c_{23} & -c_{13} \\
c_{17}^* & 0 & -c_{26}^* & c_{25}^* + 2c_{16} & -c_{24}^* & -c_{23}^* & 0 & -c_{12} \\
0 & -c_{17}^* & -c_{16}^* & c_{15}^* - 2c_{26} & -c_{14}^* & -c_{13}^* & -c_{12}^* & 0
\end{bmatrix}.$$

It follows that from the fact that the submatrix formed by fourth and fifth columns has rank exactly 1, we have $c_{14}(-c_{14}^*) = c_{15}(c_{15}^* - 2c_{26})$. Thus at least one of the following cases must happen.

(10.1) $c_{14} = c_{15} = 0$. We can still assume there is no column containing only zero elements as this is the case that we have already discussed. Thus $c_{26} = 0$ which would also lead to $c_{23} = 0$.

(10.2) $c_{26} = c_{15}^*$.

Similarly, at least one of the following conditions: (10.I) $c_{24} = c_{25} = c_{16} = c_{13} = 0$ or (10.II) $c_{16} = -c_{25}^*$ and one of the following conditions: (10.A) $c_{34} = c_{35} = c_{17} = c_{12} = 0$ or (10.B) $c_{17} = c_{35}^*$ must apply.

We have already discussed the cases that $c_{12} = c_{17} = 0$, $c_{13} = c_{16} = 0$, or $c_{23} = c_{26} = 0$ previously. Hence the only remaining case is $c_{26} = c_{15}^*, c_{16} = -c_{25}^*, c_{17} = c_{35}^*$. Thus

$$H = \begin{bmatrix}
0 & c_{12} & c_{13} & c_{14} & c_{15} & -c_{25}^* & c_{35}^* & 0 \\
c_{12}^* & 0 & c_{23} & c_{24} & c_{25} & c_{15}^* & 0 & -c_{35}^* \\
c_{13}^* & c_{23}^* & 0 & c_{34} & c_{35} & 0 & -c_{15}^* & c_{25}^* \\
c_{14}^* & c_{24}^* & c_{34}^* & 0 & 0 & -c_{35} & -c_{25} & -c_{15} \\
c_{15}^* & c_{25}^* & c_{35}^* & 0 & 0 & -c_{34} & -c_{24} & -c_{14} \\
-c_{25} & c_{15} & 0 & -c_{35}^* & -c_{34}^* & 0 & -c_{23} & -c_{13} \\
c_{35} & 0 & -c_{15} & -c_{25}^* & -c_{24}^* & -c_{23}^* & 0 & -c_{12} \\
0 & -c_{35} & c_{25} & -c_{15}^* & -c_{14}^* & -c_{13}^* & -c_{12}^* & 0
\end{bmatrix}.$$

According to $c_{26} = c_{15}^*$, we have $2(b_2 + b_3)(1 - 4b_1b_4) = (4b_2b_3 - 1)(2b_1 + 2b_4)$, which implies $4(b_1b_2b_3 + b_1b_2b_4 + b_1b_3b_4 + b_2b_3b_4) = b_1 + b_2 + b_3 + b_4$.

(1) $4b_1b_2 + 4b_1b_3 + 4b_2b_3 = 1$. Thus $b_1 + b_2 + b_3 = 4b_1b_2b_3$. However, one can easily verify that there do not exist three real numbers b_1, b_2, b_3 satisfying these two equations.

(2) $4b_1b_2 + 4b_1b_3 + 4b_2b_3 \neq 1$. Hence $b_4 = \frac{b_1+b_2+b_3-4b_1b_2b_3}{4b_1b_2+4b_1b_3+4b_2b_3-1}$. By substituting the assignment of b_4 into Eq. (A10), we have

$$
\begin{aligned}
c_{14} &= p \cdot \left(\frac{2\left(1 - 4b_1^2\right)(b_2 + b_3) + 4b_1(1 - 4b_2b_3)}{4b_1b_2 + 4b_1b_3 + 4b_2b_3 - 1} + \frac{-8b_1(b_2 + b_3) + \left(1 - 4b_1^2\right)(1 - 4b_2b_3)}{4b_1b_2 + 4b_1b_3 + 4b_2b_3 - 1} i \right), \\
c_{15} &= p \cdot \left(\frac{2\left(1 + 4b_1^2\right)(b_2 + b_3)}{4b_1b_2 + 4b_1b_3 + 4b_2b_3 - 1} + \frac{\left(1 + 4b_1^2\right)(1 - 4b_2b_3)}{4b_1b_2 + 4b_1b_3 + 4b_2b_3 - 1} i \right), \\
c_{23} &= p \cdot \left(\frac{2\left(1 + 4b_1^2\right)(b_3 - b_2)}{4b_1b_2 + 4b_1b_3 + 4b_2b_3 - 1} + \frac{\left(1 + 4b_1^2\right)(1 + 4b_2b_3)}{4b_1b_2 + 4b_1b_3 + 4b_2b_3 - 1} i \right), \\
c_{24} &= q \cdot \left(\frac{2\left(1 - 4b_2^2\right)(b_1 + b_3) + 4b_2(1 - 4b_1b_3)}{4b_1b_2 + 4b_1b_3 + 4b_2b_3 - 1} + \frac{8b_2(b_1 + b_3) - \left(1 - 4b_2^2\right)(1 - 4b_1b_3)}{4b_1b_2 + 4b_1b_3 + 4b_2b_3 - 1} i \right), \\
c_{25} &= q \cdot \left(\frac{2\left(1 + 4b_2^2\right)(b_1 + b_3)}{4b_1b_2 + 4b_1b_3 + 4b_2b_3 - 1} + \frac{\left(1 + 4b_2^2\right)(1 - 4b_1b_3)}{4b_1b_2 + 4b_1b_3 + 4b_2b_3 - 1} i \right), \\
c_{13} &= q \cdot \left(\frac{2\left(1 + 4b_2^2\right)(b_1 - b_3)}{4b_1b_2 + 4b_1b_3 + 4b_2b_3 - 1} - \frac{\left(1 + 4b_2^2\right)(1 + 4b_1b_3)}{4b_1b_2 + 4b_1b_3 + 4b_2b_3 - 1} i \right), \\
c_{34} &= r \cdot \left(\frac{2\left(1 - 4b_3^2\right)(b_1 + b_2) + 4b_3(1 - 4b_1b_2)}{4b_1b_2 + 4b_1b_3 + 4b_2b_3 - 1} + \frac{8b_3(b_1 + b_2) - \left(1 - 4b_3^2\right)(1 - 4b_1b_2)}{4b_1b_2 + 4b_1b_3 + 4b_2b_3 - 1} i \right), \\
c_{35} &= r \cdot \left(\frac{2\left(1 + 4b_3^2\right)(b_1 + b_2)}{4b_1b_2 + 4b_1b_3 + 4b_2b_3 - 1} + \frac{\left(1 + 4b_3^2\right)(1 - 4b_1b_2)}{4b_1b_2 + 4b_1b_3 + 4b_2b_3 - 1} i \right), \\
c_{12} &= r \cdot \left(\frac{2\left(1 + 4b_3^2\right)(b_2 - b_1)}{4b_1b_2 + 4b_1b_3 + 4b_2b_3 - 1} + \frac{\left(1 + 4b_3^2\right)(1 + 4b_1b_2)}{4b_1b_2 + 4b_1b_3 + 4b_2b_3 - 1} i \right).
\end{aligned}
$$

Again, with the assistance of symbolic computation package like Mathematica, we can verify that the characteristic polynomial of H contains only even powers. This implies H has nonzero eigenvalue λ if and only if it also has eigenvalue $-\lambda$. Therefore, under our assumption that H has only one positive eigenvalue, H also has only one negative eigenvalue.

However, let us consider the 3×3 submatrix of H formed by (5,7,8)th rows and (1,2,3)th columns. Its determinant is $(-i + 2b_1)(i + 2b_1)^2(1 + 2ib_2)(i + 2b_2)^2(i - 2b_3)^2(i + 2b_3)^2 r((1 + 4b_1^2)p^2 + (1 + 4b_2^2)q^2 + (1 + 4b_3^2)r^2)$. It is always nonzero unless $p = q = r$ or $r = 0$. If $r = 0$ this implies that $c_{12} = c_{34} = c_{35} = 0$. This case has already been covered. Thus H has rank at least 3 which contradicts our previous conclusion that H has only one positive eigenvalue and only one negative eigenvalue.

To summarize, under our assumption that H has only one positive eigenvalue, a contradiction always exists in every situation we studied. Hence H must have at least two positive eigenvalues and at least two negative eigenvalues. This completes our proof.

APPENDIX B: FIDELITY COMPARISON IN THE TWO-QUBIT NMR EXPERIMENT

The Hamiltonian in the two-qubit NMR experiment is shown in Eq. (10), and the system will evolve to a time-dependent state shown in Eq. (11). To test the stability of our protocol against purities, we choose a long evolution time which results in a tremendous drop in purities. In Fig. 9, we compare two fidelities: the fidelity between the aim pure state and the reconstructed state by 16 Pauli measurements

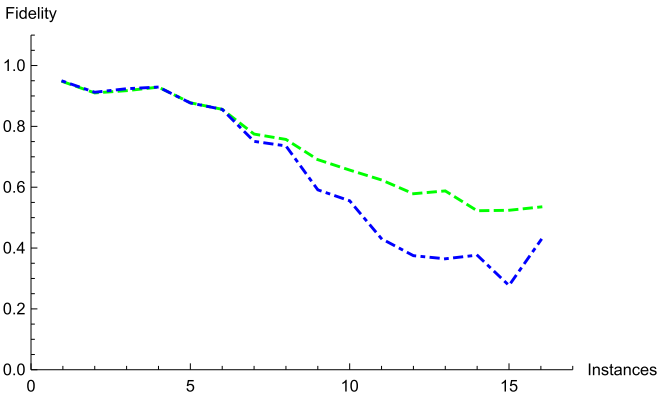

FIG. 9. Fidelity of the different reconstructions against the state intended to be prepared. The green dashed line show the fidelity between the aim pure state and the reconstructed state by 16 Pauli measurements, and the blue dash-dotted line shows the fidelity between the aim pure state and the reconstructed state by 11 Pauli measurements in our protocol. Both of them decrease when the purity is low, as our truly prepared state becomes more and more mixed along with the long evolution times. For low purities, our protocol is also worse than full-state tomography.

which is full-state tomography, and the fidelity between the aim pure state and the reconstructed state by 11 Pauli measurements in our protocol. We can see that for short evolution times, these two fidelities are almost the same, but for low purities, the fidelity of our protocol is less than the fidelity of full-state tomography. It clearly shows that our protocol is only valid for high purities when the state is close to pure.

[1] D. F. V. James, P. G. Kwiat, W. J. Munro, and A. G. White, Phys. Rev. A **64**, 052312 (2001).

[2] M. D. de Burgh, N. K. Langford, A. C. Doherty, and A. Gilchrist, Phys. Rev. A **78**, 052122 (2008).

[3] L. M. Vandersypen and I. L. Chuang, Rev. Mod. Phys. **76**, 1037 (2005).

[4] I. Oliveira, R. Sarthour, Jr., T. Bonagamba, E. Azevedo, and J. C. Freitas, *NMR Quantum Information Processing* (Elsevier, Amsterdam, 2011).

[5] M. Nielsen and I. Chuang, *Quantum Computation and Quantum Information* (Cambridge University Press, Cambridge, England, 2000).

[6] J. Chen, H. Dawkins, Z. Ji, N. Johnston, D. Kribs, F. Shultz, and B. Zeng, Phys. Rev. A **88**, 012109 (2013).

[7] T. Heinosaari, L. Mazzarella, and M. M. Wolf, Commun. Math. Phys. **318**, 355 (2013).

[8] S. Weigert, Phys. Rev. A **45**, 7688 (1992).

[9] J.-P. Amiet and S. Weigert, J. Phys. A: Math. Gen. **32**, 2777 (1999).

[10] J. Finkelstein, Phys. Rev. A **70**, 052107 (2004).

[11] S. T. Flammia, A. Silberfarb, and C. M. Caves, Found. Phys. **35**, 1985 (2005).

[12] N. Li, C. Ferrie, and C. M. Caves, arXiv:1507.06904.

[13] C. H. Baldwin, I. H. Deutsch, and A. Kalev, arXiv:1510.02736.

[14] A. Kalev and C. H. Baldwin, arXiv:1511.01433.

[15] C. Carmeli, T. Heinosaari, J. Schultz, and A. Toigo, Eur. Phys. J. D **69**, 179 (2015).

[16] D. Gross, Y.-K. Liu, S. T. Flammia, S. Becker, and J. Eisert, Phys. Rev. Lett. **105**, 150401 (2010).

[17] M. Cramer, M. B. Plenio, S. T. Flammia, R. Somma, D. Gross, S. D. Bartlett, O. Landon-Cardinal, D. Poulin, and Y.-K. Liu, Nat. Commun. **1**, 149 (2010).

[18] A. Kalev, R. L. Kosut, and I. H. Deutsch, npj Quantum Inf. **1**, 15018 (2015).

[19] W.-T. Liu, T. Zhang, J.-Y. Liu, P.-X. Chen, and J.-M. Yuan, Phys. Rev. Lett. **108**, 170403 (2012).

[20] T. Jackson, Master's thesis, University of Guelph, Canada, 2013.

[21] D. G. Cory, A. F. Fahmy, and T. F. Havel, Proc. Natl. Acad. Sci. USA **94**, 1634 (1997).

[22] D. Lu, A. Brodutch, J. Park, H. Katiyar, T. Jochym-O'Connor, and R. Laflamme, arXiv:1501.01353.

[23] X. Peng, J. Du, and D. Suter, Phys. Rev. A **71**, 012307 (2005).

[24] Y. Gao, H. Zhou, D. Zou, X. Peng, and J. Du, Phys. Rev. A **87**, 032335 (2013).

[25] J. B. Altepeter, E. R. Jeffrey, and P. G. Kwiat, Opt. Express **13**, 8951 (2005).

[26] R. Prevedel, P. Walther, F. Tiefenbacher, P. Bohi, R. Kaltenbaek, T. Jennewein, and A. Zeilinger, Nature (London) **445**, 65 (2007).

[27] K. Chen, C.-M. Li, Q. Zhang, Y.-A. Chen, A. Goebel, S. Chen, A. Mair, and J.-W. Pan, Phys. Rev. Lett. **99**, 120503 (2007).

[28] R. Prevedel, D. R. Hamel, R. Colbeck, K. Fisher, and K. J. Resch, Nat. Phys. **7**, 757 (2011).

[29] C. Erven, E. Meyer-Scott, K. Fisher, J. Lavoie, B. L. Higgins, Z. Yan, C. J. Pugh, J.-P. Bourgoin, R. Prevedel, L. K. Shalm, L. Richards, N. Gigov, R. Laflamme, G. Weihs, T. Jennewein, and K. J. Resch, Nat. Photon. **8**, 292 (2014).

[30] D. R. Hamel, L. K. Shalm, H. Hübel, A. J. Miller, F. Marsili, V. B. Verma, R. P. Mirin, S. W. Nam, K. J. Resch, and T. Jennewein, Nat. Photon. **8**, 801 (2014).

[31] R. B. A. Adamson and A. M. Steinberg, Phys. Rev. Lett. **105**, 030406 (2010).

[32] R. A. Horn and C. R. Johnson, *Matrix Analysis* (Cambridge University Press, Cambridge, UK, 2012).